Final Draft
of the original manuscript:

Wierzbicka-Miernik, A.; Wojewoda-Budka, J.; Miernik, K.;
Litynska-Dobrzynska, L.; Schell, N.:

Characteristics of intermetallic phases in Cu/(Sn,Ni) diffusion couples annealed at 220 °C

In: Journal of Alloys and Compounds (2016) Elsevier

DOI: 10.1016/j.jallcom.2016.09.147

Characteristics of intermetallic phases in Cu/(Sn,Ni) diffusion couples annealed at 220 °C

A. Wierzbicka-Miernik[1,*], J. Wojewoda-Budka[1], K. Miernik[2], L. Litynska-Dobrzynska[1], N. Schell[3]

[1] Institute of Metallurgy and Materials Science, Polish Academy of Sciences,

25 Reymonta St., 30-059 Cracow, Poland

[2] Institute of Materials Engineering, Cracow University of Technology,

37 Jana Pawla II Av., 31-866 Cracow, Poland

[3] Institute of Materials Research, Helmholtz-Zentrum Geesthacht, Max-Planck-Strasse 1,

D-21502 Geesthacht, Germany

[*] Corresponding author: a.wierzbicka@imim.pl

Abstract

The influence of Ni addition (5 at.%) on the morphology and chemical composition of the phases formed during solid state reaction in Cu/(Sn,Ni) diffusion couples, annealed at 220 °C for different periods of time, was investigated. Chemical analysis of the reaction zone performed using scanning electron microscopy (SEM/EDS) identified several intermetallic phases. Near to the copper substrate, a thin and continuous layer of the Cu_3Sn phase was observed. Moving towards the (Sn,Ni) end of the diffusion couple, the $(Cu_{1-x}Ni_x)_6Sn_5$ phase was identified. This phase was represented by two types of structures: a discontinuous layer located close to the Cu_3Sn phase, and precipitates (needles or faced) within the (Sn,Ni) end. These structures of $(Cu_{1-x}Ni_x)_6Sn_5$ also varied in chemical composition. The experiment with synchrotron radiation demonstrated two crystallographic variants of the Cu_6Sn_5 phase: high-temperature hexagonal η and low-temperature monoclinic η′; however, only the hexagonal variant was confirmed by TEM. Differences in the morphology and chemical composition of the $(Cu_{1-x}Ni_x)_6Sn_5$ phase were attributed to various mechanisms of their formation. The precipitates with a higher content of Ni were most probably transformed from the Ni_3Sn_4 phase present in the initial (Ni,Sn) end-member, while the formation of the Ni-poor layer took place as a result of diffusion at the initial interface. After the annealing experiment, the $(Ni_{1-x}Cu_x)_3Sn_4$ phase was observed beyond the interface area as small, irregularly distributed precipitates in the (Sn,Ni) end-member. TEM examination allowed for the precise phase characterisation of the mentioned intermetallics. Moreover, except for the strong reflections visible in SADP fitted to the hexagonal η-Cu_6Sn_5 phase, additional reflections were observed and assigned to the cubic Cu_9NiSn_3 phase.

Keywords: intermetallics; solid state reactions; microstructure; scanning electron microscopy; synchrotron radiation; transmission electron microscopy

1. Introduction

Studies of Cu/Sn diffusion couples [1] and Cu/Sn/Cu diffusion soldered joints [2,3] have showed that Ni addition (up to 5 at.%) to the copper substrate changed not only the morphology but also the sequence of intermetallic phases (IP) growing in the reaction zone. Chemical composition analyses at the interface have revealed the presence of only one phase $(Cu,Ni)_6Sn_5$ in both systems. No ε-Cu_3Sn was detected as opposed to the conventional Cu/Sn diffusion couples [1,4] and Cu/Sn/Cu interconnections [3,5,6], in which both these phases were observed. When no Ni was added to the copper, ε-Cu_3Sn appeared as a thin, irregular interlayer between copper and η-Cu_6Sn_5. The addition of nickel to the Cu caused the $(Cu_{1-x}Ni_x)_6Sn_5$ phase to form and grow in the entire reaction zone [2], which was substantially different from the conventional Cu/Sn diffusion couples [1,4] and Cu/Sn/Cu interconnections [3], in which the phase appeared as a continuous, irregular layer and as scallops from the Cu substrate towards the reaction zone centre, respectively. Furthermore, the fraction of the tin solder that transformed into $(Cu_{1-x}Ni_x)_6Sn_5$ intermetallic compound (IMC) was larger [7] than that of η-Cu_6Sn_5 in the Cu/Sn/Cu [3] samples. A similar observation was made by Paul [1] for Cu 5–25 at. %Ni/Sn diffusion couples annealed at 215 °C for 400 h.

Such significant changes of the $(Cu,Ni)_6Sn_5$ growth kinetics may be very promising in the sense of a diffusion soldering technique, in which the goal of the process is the presence of intermetallic phase(s) totally fulfilling the interconnection area. On the other hand, the absence of the Cu_3Sn phase often decorated with Kirkendall voids can be beneficial in the classical soldering process. Despite these two advantages, the addition of nickel into copper may be difficult in everyday practice; therefore, studies concerning its influence when it is added into tin (solder) would be of great importance. Our previous studies were related to the Cu/(Sn,Ni) diffusion couples experiment, in which 1 and 5 at.% of nickel were added to the tin substrates. The microstructural observations and chemical composition analysis of the investigated diffusion couples, after annealing at 215 °C for different times, revealed the presence of three intermetallic compounds (IMCs) that were located in the following order, from the (Sn,Ni) pad towards Cu: $(Ni_{1-x}Cu_x)_3Sn_4$; $(Cu_{1-x}Ni_x)_6Sn_5$; and finally, Cu_3Sn [8]. The $(Cu_{1-x}Ni_x)_6Sn_5$ phase had a dual morphology. Close to the (Sn,Ni) pad, the grains were needle-like and had faced shapes surrounded by pure tin. Next to the Cu_3Sn phase, which grew as an irregular but continuous layer [8], a discontinuous layer of $(Cu_{1-x}Ni_x)_6Sn_5$ was present. The significant differences in the chemical composition within the $(Cu_{1-x}Ni_x)_6Sn_5$ phase were related to its location and morphology.

Therefore, the purpose of this study is an intensive investigation of the addition of nickel to tin, and its influence on the morphology and chemical composition of the IMCs growing in the Cu/(Sn,Ni) diffusion couples with the 5 at.% of Ni content, annealed in a vacuum at 220 °C for different periods of time.

2. Experimental

The pure metals Sn 99.998%, Ni 99.99 % and Cu 99.99 % (Alfa Aesar) were used to prepare the substrates (Sn,Ni) and Cu for the diffusion couple experiment.
The pads (Sn,Ni) with 5 at.% of Ni (Sn+5 at.% Ni) and Cu were prepared by melting appropriate amounts of pure metals in a vacuum induction furnace (Leybold-Heraeus) under an argon protective atmosphere (0.03 MPa). The melting temperatures were selected such that they exceeded the liquidus temperature of about 100 °C. In the next step, the liquid (Sn,Ni) alloy and Cu were cast into the steel mould (internal dimensions: 90 mm x 15 mm).
The pads (Sn,Ni) and Cu, with a thickness of 3 mm, were cut from the cast alloys, and their surfaces were prepared first by grinding using paper with a maximum gradation of 2000, then cleaned with acetone in an ultrasonic washer before annealing.
The diffusion couples were pressed and sealed in quartz ampoules. They were further subjected to annealing at 220 °C (493 K) for different times of 48, 120 and 168 hours, followed by cooling in a furnace for an appropriate time interval.
The microstructure and chemical composition analyses of the diffusion couple cross-sections were performed using the scanning electron microscope JEOL JSM 5510 LV equipped with an energy dispersive X-ray spectrometer (EDS), IXRF Model 500.
The phase analysis of the entire diffusion couple was performed using diffraction of high-energy synchrotron radiation (87.1 keV, λ=0.014235 nm, beamline P07 at DESY in Hamburg, Germany). Data were collected with the beam size of 0.8 mm × 0.8 mm using an area detector, placed at a distance of 1050 mm from the sample. The samples subject to radiation were first polished on each side using abrasive papers (ending with P4000). The sample was irradiated along the Cu/(Sn,Ni) interface; during the measurement, it was continuously rotated around the ω axis from − 90° to 90°, perpendicular to the interface.
Further characteristics, comprising the microstructure, chemical composition changes and the phase analysis, were carried out on the transmission electron microscope TECNAI FEI, G2 FEG/200 kV (TEM/HRTEM) equipped with a High-Angle Annular Dark Field (HAADF) detector and integrated with an energy dispersive X-ray spectrometer (EDS, Phoenix type) manufactured by the EDAX company. The thin foils were prepared using the focused ion beam (FIB) technique with Quanta 3D (FEI).

3. Results and Discussion

The SEM microstructural observations of the Cu/(Sn+5 at.% Ni) diffusion couples annealed at 220 °C for 48, 120 and 168 hr revealed the complex morphology of the interface compared to the classical Cu/Sn couples (Fig. 1). Regardless of the time of interaction, the microstructure did not change in the sense of the phase composition; but the amount of the phases slightly differed. The EDS chemical analysis identified three intermetallic phases in the reaction zone. The thin continuous layer near to the Cu pad consisted of 74.7±1.5 at. % of Cu and 25.3±0.5 at.% of Sn, which undoubtedly could be identified as the Cu_3Sn phase (Fig. 1, point 1). The next two phases belonged chemically to the $(Cu_{1-x}Ni_x)_6Sn_5$ phase. The chemical composition of such a dual morphology can be described as Ni-poor (49.3±1.0 at.% of Cu, 4.0 ± 0.5 at.% of Ni and 46.7±0.9 at.% of Sn, Fig. 1, point 2) layer and the Ni-rich

(31.3±0.6 at.% of Cu, 22.4 ± 0.9 at.% of Ni and 46.3±0.9 at.% of Sn, Fig. 1, point 3) one in the form of needles or faced precipitates. The differences in the nickel concentrations of the $(Cu_{1-x}Ni_x)_6Sn_5$ phase can be followed along the SEM/EDS linescan presented in Fig. 2. Additionally, the Kirkendall phenomenon was manifest in the investigated diffusion couples by voids formed across the line within the $(Cu_{1-x}Ni)_6Sn_5$ phase, and at the Cu-Cu_3Sn interface (Figs. 1b,d).

Moreover, in all the prepared diffusion couples, beyond the interface area (up to 200 μm in the Sn matrix), small precipitates were identified as $(Ni_{1-x}Cu_x)_3Sn_4$ (see example in Fig. 1a) with the following concentration: 7.4 ±1.5 at.% of Cu, 33.2 ±1.3 at.% of Ni, 59.4 ±1.1 at.% of Sn close to the reaction zone (Fig. 1, point 4), and 3.4± 0.4 at.% of Cu, 39.2 ±0.8 at.% of Ni, 57.4 ±1.1 at.% of Sn far from the Cu/(Sn,Ni) interface (Fig. 1, point 5). The presence of the $(Ni_{1-x}Cu_x)_3Sn_4$ phase resulted from the diffusion of copper into the already-existing Ni_3Sn_4 phase within the pad before the diffusion couple experiment [8].

Furthermore, the light grey areas surrounded by the Ni-rich variant of the $(Cu_{1-x}Ni_x)_6Sn_5$ phase (black circle in Fig. 2a) were observed in the SEM micrographs of the diffusion couple annealed for the longest time of annealing, i.e. 168 hours. The phase of such a contrast was not observed in the case of the samples prepared at 215 °C and described in detail elsewhere [8]. Based on the SEM/EDS linescan results (Fig. 2b), it became clear that the tin concentration sharply increased within that phase, with a simultaneous minor decrease in the Ni content. Unfortunately, the SEM/EDS measurements were doubtful, due to the insufficient analytical resolution (area of interest smaller than 1 μm).

Moreover, the dual morphology and fluctuations in the chemical composition of the $(Cu_{1-x}Ni_x)_6Sn_5$ phase have also been described by Nakayama et al. [9] in the case of the Cu/(Sn,Ni) diffusion couples with 1 and 3 at.% of the nickel addition annealed at 160, 180 and 200 °C for various durations up to 1139.5 h, where three intermetallic phases were generally observed in the reaction zone. The chemical composition analyses were performed with the EPMA method. The results revealed that the Cu_3Sn phase was formed close to the Cu pad as the thin and continuous layer, like in our diffusion couples. The second layer, farther from Cu, was defined as the Cu_6Sn_5 phase. Furthermore, the single detached grains present in the Sn-Ni pad were identified as $(Cu,Ni)_6Sn_5$. The dual morphology and fluctuations of the Ni concentration could have resulted from the different mechanisms of their growth. Nakayama et al. [9] suggested that the $(Cu,Ni)_6Sn_5$ phase appeared due to the transformation from the Ni_3Sn_4 phase, which was also present in the Sn-Ni end-member before the diffusion couple experiment. The transformation took place because of the diffusion of copper into the Sn-Ni alloy; however, no evidence for such a transformation was presented [9].

Further phase analyses of the Cu/(Sn+5 at.%Ni) diffusion couples were performed using the synchrotron radiation and selected area electron diffraction in the transmission electron microscope. The X-ray synchrotron diffraction presented in Fig. 3a mainly shows the reflections coming from the two end-members of the diffusion couple (copper and tin with nickel addition). In order to reveal the phase composition of their interface, inspection with a different intensity scale at the central part of the diffraction pattern (Fig. 3b) was performed; the data are collected in Table 1. In general, the EDS analysis was supported by the phase analysis based on the synchrotron experiment. However, it should be emphasised that the Cu_6Sn_5 phase was identified in both allotropic structures: the low-temperature monoclinic η′

and high-temperature η hexagonal one. Their transformation temperature according to the Cu-Sn equilibrium phase diagram is 186 °C. Literature data related to the interconnection reliability indicate the volumetric change of 2.15 % occurring during the η′→η transformation as that responsible for the crack propagation at the solder/pad interface [10]. The addition of nickel can act as the stabiliser of the high-temperature η-Cu_6Sn_5 phase, minimising the transformation during service of the electronic equipment. The presence of the monoclinic η′ phase in the studied Cu/(Sn,Ni) diffusion couples is related to the low cooling rate after the experiment (with a furnace), ensuring sufficient time for the transformation η→η' to take place.

The second phase, identified as the Cu_3Sn phase, formed at the interface and composed of 74.7 at. % of Cu and 25.3 at% of Sn, was also evidenced by the synchrotron experiment, showing orthorhombic symmetry (ε).

Table 1. Phase identification based on synchrotron radiation experiment for Cu/(Sn,Ni) diffusion couple presented in Fig. 3.

Ring number in Fig. 3b	Phase	Plane	Experimental d_{hkl}, [nm]	Theoretical d_{hkl} [nm]	Lattice parameters [nm]	Ref.
1	Ni_3Sn_4	[200]	0.586	0.589	a=1.2199, b=0.40609, c=0.52238, β=105.17°	[11]
2	η′–Cu_6Sn_5	[110]	0.561	0.559	a=0.984, b=0.727, c=0.984, α,γ=90°, β=117.5°	[12]
3	η′–Cu_6Sn_5	[111]	0.418	0.418		
4	η′–Cu_6Sn_5	[11-2]	0.405	0.407		
5	η–Cu_6Sn_5	[100]	0.364	0.363	a=0.4192, c=0.5037, γ=120°	[13]
6	Cu_3Sn	[110]	0.333	0.339	a=0.549, b=0.432, c=0.474	[13]
7	Ni_3Sn_4	[111]	0.298	0.294	a=1.2199, b=0.40609, c=0.52238, β=105.17°	[11]
8	Ni_3Sn_4	[40-1]	0.292	0.289		
9	Ni_3Sn_4	[310]	0.280	0.282		
10	Sn	[110]	0.262	0.262	a=b=0.37, c=0.337, α,β,γ=90°	[14]
11	Ni_3Sn_4	[20-2]	0.256	0.257	a=1.2199, b=0.40609, c=0.52238, β=105.17°	[11]
12	Sn	[101]	0.241	0.249	a=b=0.37, c=0.337, α,β,γ=90°	[14]
13	Cu_3Sn	[020]	0.218	0.216	a=0.549, b=0.432, c=0.474	[13]
14	Cu_3Sn	[211]	0.209	0.208		
15	η–Cu_6Sn_5	[102]	0.203	0.207	a=0.4192,	[13]

					c=0.5037, γ=120°	
16	Cu	[200]	0.181	0.181	a=b=c=0.3615, α,β,γ=90°	[15]

TEM investigations of the studied diffusion couples were conducted to obtain more detailed information concerning the microstructure and phase composition. Figure 4a presents the areas selected from the Cu/(Sn+5at.% Ni) diffusion couple annealed for 168 hours for the preparation of thin foils by the FIB technique (Figs. 4b,c).

The results of the TEM examination of area 1 located at Cu/(Sn+5 at. % Ni) (in Fig. 4) are shown in Fig. 5. Based on the EDS/TEM mappings (Figs. 5b-d) obtained for the area marked in the STEM image in Fig. 5a, no increase of the Ni content near the reaction zone was observed, as when nickel was added to the copper in (Cu,Ni)/Sn/(Cu,Ni) diffusion soldered joints [2]. In that case, such a Ni enrichment at the substrate/reaction zone interface acted as the diffusion barrier, and was responsible for the lack of the ε-Cu_3Sn phase at the interface [2]. In Figs. 5a and 5e, next to the copper, a row of columnar grains of about 3 x 1 μm in size is clearly visible. Based on the selected area diffraction patterns (SADP), these grains were identified as the orthorhombic ε-Cu_3Sn phase. As an example, Fig. 5f shows the SADP with [102] zone axis corresponding to the area marked in Fig. 5e. The examples of large grains (with the mottled contrast) lying in the vicinity of the ε-Cu_3Sn phase are shown in Figs. 5g,i. The inserts in Figs. 5g,i present the microstructure under higher magnification. The SADP obtained for the first presented grain was indexed as the monoclinic Ni_3Sn_4 phase with [001] zone axis (marked in Fig. 5h in yellow). The strong reflections visible in that SADP could be fitted with a high accuracy to the hexagonal η-Cu_6Sn_5 phase (marked in white). The orientation relationship between these phases determined from the presented SADP is $[0001]\eta \parallel [001]Ni_3Sn_4$ and $(03\text{-}30)\eta \parallel (200)\ Ni_3Sn_4$. Very weak reflexes were additionally found in the SADP corresponding to the next grain (Fig. 5j, marked in blue), which were assigned to cubic Cu_9NiSn_3 with a [111] zone axis. The following orientation relationship was found for this phase and hexagonal η-Cu_6Sn_5: $[0001]\eta \parallel [111]Cu_9NiSn_3$ and $(11\text{-}20)\eta \parallel (\text{-}220)Cu_9NiSn_3$. All the presented SADPs suggest a strong relationship between the identified phases, confirming the role of the Ni_3Sn_4 phase in the formation of the η-Cu_6Sn_5 phase. The reflexes corresponding to the Cu_9NiSn_3 phase with a cubic face-centered structure with a=1.8011 nm [13] were not previously observed in the case of the Cu/(Sn,Ni) diffusion couples annealed at a lower temperature of 215 ºC [8]. Deraisme et al. [16] suggested that the Cu_9NiSn_3 phase (denoted there as cubic δ of cF416 point group symmetry) may be a super cell of Cu_3Sn (cubic γ of cF16 point group symmetry), which opens the possibility of an easy $\gamma \leftrightarrow \delta$ transformation. A very detailed crystallographic description of the Cu_9NiSn_3 phase was also presented by Booth et al. [17].

Figure 6 shows the STEM image and EDS/TEM mapping (Figs. 6a-d), the bright field images (Figs. 6e,g) and the corresponding selected area diffraction patterns (Figs. 6f, h-j) of the area placed farther from the interface Cu/(Sn,Ni) and marked as 2 in Fig. 4. The SADP obtained for the light grey region (black circle in Fig. 2a) is referred to as the Ni_3Sn_4 intermetallic phase (Fig. 6f). The TEM chemical composition analysis additionally revealed the presence of copper within the Ni_3Sn_4 phase. The grains surrounding the Ni_3Sn_4 phase, enriched in Ni, could be identified as the hexagonal η-Cu_6Sn_5 phase (strong reflections in SADPs in Figs. 6h-

j). Again, as it was in the first location studied in TEM, additional reflections were assigned to the cubic Cu_9NiSn_3 phase. The SADP corresponding to the bright field image in Fig. 6g with [011] Cu_9NiSn_3 zone axis is presented in Fig. 6h. The positions of the strong reflections related to the η-Cu_6Sn_5 phase demonstrate the following crystallographic relationships between these phases: [2-1-10]η ‖ [011]Cu_9NiSn_3 and (0-111)η ‖ (200) Cu_9NiSn_3. Several SADPs obtained for various grains confirmed the presence of the weak reflexes characteristic of Cu_9NiSn_3 , as well as its crystallographic relationship to the hexagonal η-Cu_6Sn_5 phase. Two examples of SADPs are presented in Figs. 6i, j.

Figure 7a shows a high-resolution image of a Cu_9NiSn_3 grain. The corresponding Fast Fourier Transform (FFT) pattern and the reconstructed image for the squared area in Fig. 7a are given in Figs. 7b and 7c, respectively. The periodic contrasts with an interval of three planes correspond to a distance of 0.9 nm. This distance can be assigned to the d_{002} lattice spacing of the Cu_9NiSn_3 phase.

It should be emphasised that the TEM examination only confirmed the presence of the hexagonal variant of the Cu_6Sn_5 phase. Nevertheless, the examined area was very local compared to the synchrotron experiment. Moreover, the focused ion beam preparation caused the increase in temperature within the milled material, which could contribute to the η′→η phase transformation.

4. Conclusions

The influence of 5 at. % nickel addition to tin on its reactivity with copper was interrogated at 220 °C in a diffusion couple experiment. It was found that such a modification in composition compared to the classical Cu/Sn couple was followed by a dramatic microstructural change of the interface after the annealing process. The growth of the Cu_6Sn_5 phase existing in two compositional variants – nickel-rich (dispersed within the (Sn,Ni) part of the diffusion couple), and nickel-poor (close to the initial interface) – was evidenced by SEM/EDS. Both types of phase did not form as continuous layers, but rather as islands that were more (Ni-poor) or less (Ni-rich) packed. However, they remarkably differed with respect to their grain sizes. The selected area electron diffraction pattern of the large islands of the nickel-rich variant revealed that it was formed by the transformation from the Ni_3Sn_4 phase present in the initial end member (Sn,Ni) of the diffusion couple. On the other hand, it is possible that the nickel-poor variant located near the initial Cu/(Sn,Ni) interface was created by a different mechanism: copper and tin diffusion. The synchrotron radiation experiment evidenced two crystallographic variants of the Cu_6Sn_5 phase: high-temperature hexagonal η and low-temperature monoclinic η′. Their presence was possible due to the slow cooling rate of the annealed diffusion couple, which gave sufficient time for part of the hexagonal η phase to transform into the monoclinic η′ phase. Transmission electron microscopy examination confirmed the presence of only the hexagonal Cu_6Sn_5 phase; however, apart from the fact of the very local information gathered by this technique compared to the synchrotron experiment, the focused ion beam preparation, due to temperature increase in the thin foil during milling, might have contributed to the high-temperature η phase transformation. Moreover, the high-resolution observation performed within the η phase showed the periodic

contrasts with the interval of three planes (i.e. a distance of 0.9 nm), which could be assigned to the d_{002} lattice spacing of the Cu_9NiSn_3 phase. Finally, the creation of orthorhombic ε-Cu_3Sn of continuous layer morphology located next to the copper was shown. The growth of this phase was previously reported to have been blocked by the addition of nickel to copper.

Acknowledgements

The SEM and TEM research was financially supported by the National Science Centre under grant No. 2011/03/B/ST8/06158. The TEM studies were performed in the Accredited Testing Laboratories at the Institute of Metallurgy and Materials Science of the Polish Academy of Sciences. The SEM research was carried out in the Institute of Materials Engineering, Cracow University of Technology, Poland.

References

[1] A. Paul, The Kirkendall effect in solid state diffusion. PhD thesis, Eindhoven University of Technology, Eindhoven, The Netherlands, (2004) 85–88.
[2] A. Wierzbicka-Miernik, J. Wojewoda-Budka, L. Litynska-Dobrzynska, A. Kodentsov, P. Zieba, Morphology and chemical composition of Cu/Sn/Cu and Cu(5 at-%Ni)/Sn/Cu(5 at-%Ni) interconnections, Sci. Technol. Weld. Joi. 17(1) (2012) 32–35.
[3] S. Bader, W. Gust, H. Hieber, Rapid formation of intermetallic compounds by interdiffusion in the Cu-Sn and Ni-Sn systems, Acta. Metall. Mater. 43(1) (1995) 329–337.
[4] A. Paul, A. A. Kodentsov, F. J. van Loo Intermetallic growth and Kirkendall effect manifestations in Cu/Sn andAu/Sn diffusion couples, Z. Metallkd. 95(10) (2004) 913–920.
[5] Q. Li, Y.C.Chan, Growth kinetics of the Cu_3Sn phase and void formation of sub-micrometre solder layers in Sn–Cu binary and Cu–Sn–Cu sandwich structures, J. Alloys Compd. 567 (2013) 47–53.
[6] L.D. Chen, M.L. Huang, S.M. Zhou, Effect of electromigration on intermetallic compound formation in line-type Cu/Sn/Cu interconnect, J. Alloy. Compd. 504 (2010) 535–541.
[7] A. Wierzbicka-Miernik, K. Miernik, J.Wojewoda-Budka, K. Szyszkiewicz, R. Filipek, L. Litynska-Dobrzynska, A. Kodentsov, P. Zieba, Growth kinetics of the intermetallic phase in diffusion-soldered (Cu-5 at.%Ni)/Sn/(Cu-5 at.%Ni) interconnections, Mater. Chem. Phys. 142 (2013) 682–685.
[8] A. Wierzbicka-Miernik, K. Miernik, J. Wojewoda-Budka, L. Litynska-Dobrzynska, G. Garzel, Microstructure and chemical characterization of the intermetallic phases in Cu/(Sn,Ni) diffusion couples with various Ni additions, Intermetallics, 59 (2015) 23–31.
[9] M. Nakayama, M. Kajihara, Kinetics of solid-state reactive diffusion in the (SnNi)/Cu system, Mater. Trans. 55(8) (2014) 1266–1273.
[10] K. Nogita, C.M. Gourlay, T. Nishimura, Cracking and phase stability in reaction layers between Sn-Cu-Ni solders and Cu substerates, JOM 61(6) (2009) 45–51.
[11] P. Villars, L.D. Calvert, Pearson's Handbook of crystallographic data for intermetallics phases, second edition, ASM International, Materials Park, OH, USA, 1991, vol. 4, p. 4698.
[12] A.K. Larsson, L. Stenberg, S. Lidin, Crystal structure modulations in eta-Cu_5Sn_4, Z. Kristallogr. 210 (1995) 832–837.

[13] P. Villars, L.D. Calvert, Pearson's Handbook of crystallographic data for intermetallics phases, second edition, ASM International, Materials Park, OH, USA, 1991, vol. 3.
[14] J.D. Barnett, V.E. Bean, H.T. Hall, X-ray Diffraction Studies on Tin to 100 Kilobars, J. Appl. Phys. 37 (1966) 875–877.
[15] R.P. Van Ingen, R.H.J. Fastenau, E.J Mittemeijer, Laser ablation deposition of Cu-Ni and Ag-Ni films: non-conservation of alloy composition and film microstructure, J. Appl. Phys. 76 (1994) 1871–1883.
[16] A. Deraisme, C. Servant, D. Pachoutinsky, Y. Bienvenu, J.-D. Bartout, L.-T. Mingault, P. Bertrand, R. Bailly, Cu9Ni6Sn: Determination of Phase Transformation at High Temperature, J. Phase Equilib. Diff. 31(2) (2010) 98–103.
[17] M.H. Booth, J.K. Brandon, R.Y. Brizard, C. Chien, W.B. Pearson, γ-Brasses with F cell, Acta Cryst. B33 (1977) 30–36.

Figures:

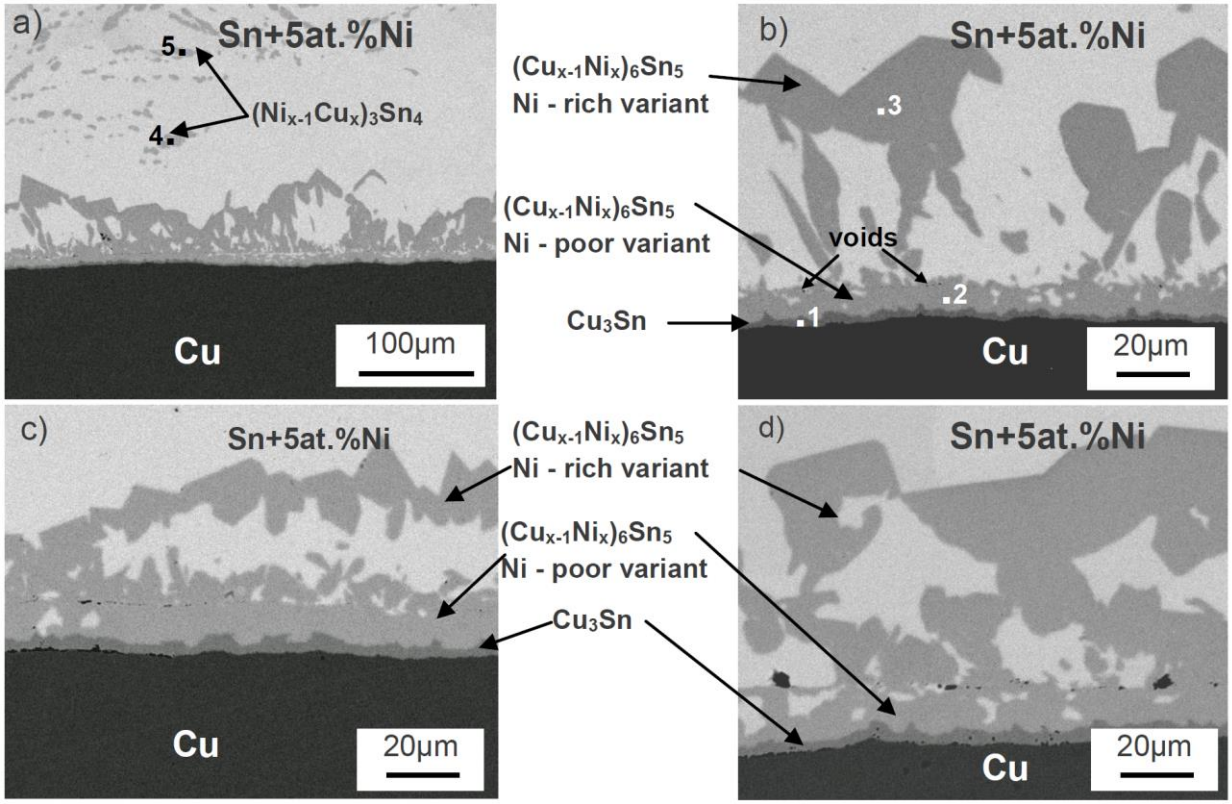

Fig. 1. SEM microstructures of Cu/(Sn+5 at.%Ni) diffusion couples annealed at 220 °C for: (a,b) 48 hours, (c) 120 hours and (d) 168 hours.

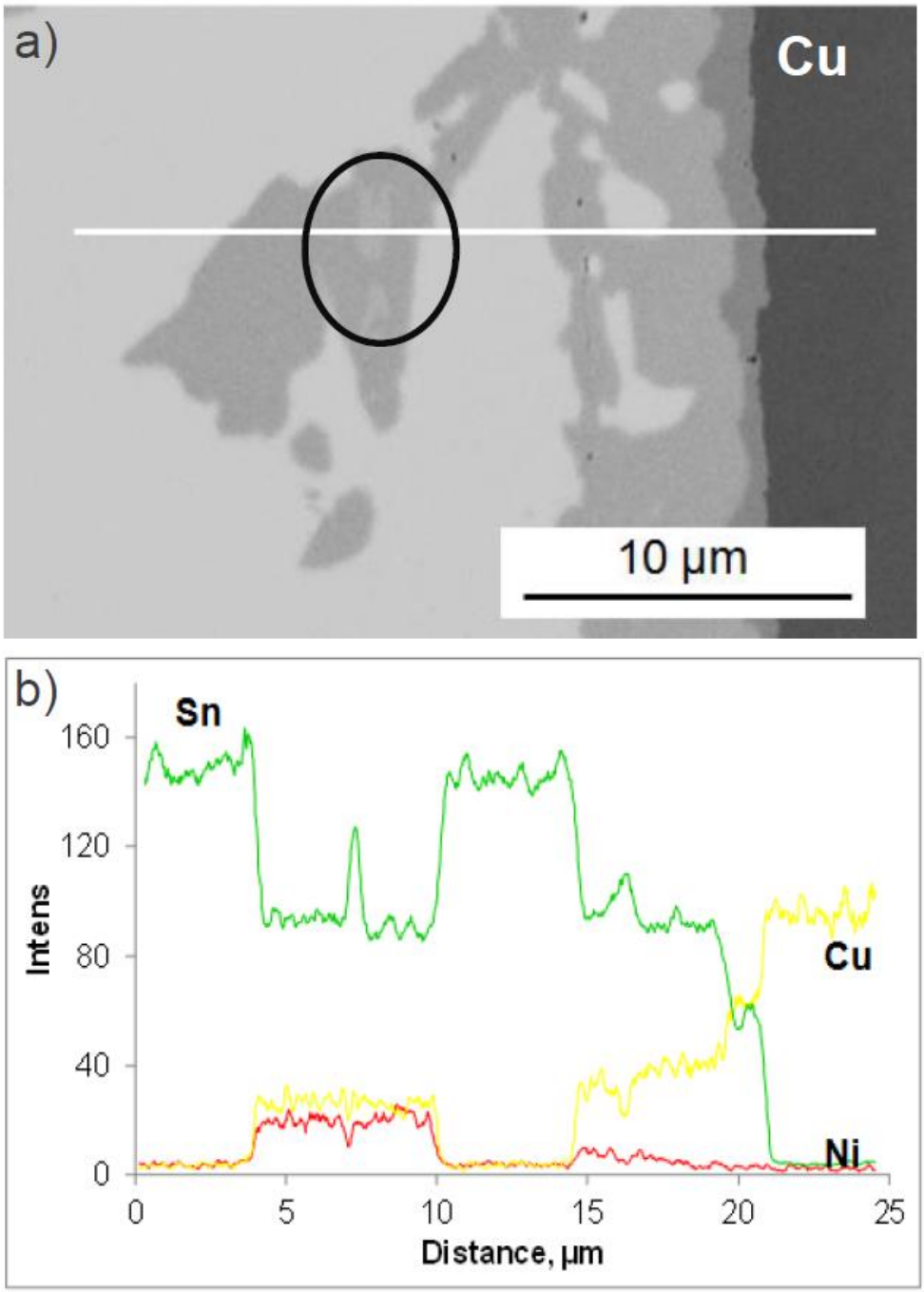

Fig. 2. (a) SEM micrograph of the Cu/(Sn+5 at.%Ni) diffusion couple annealed in a vacuum for 168 hours with (b) corresponding EDS linescan.

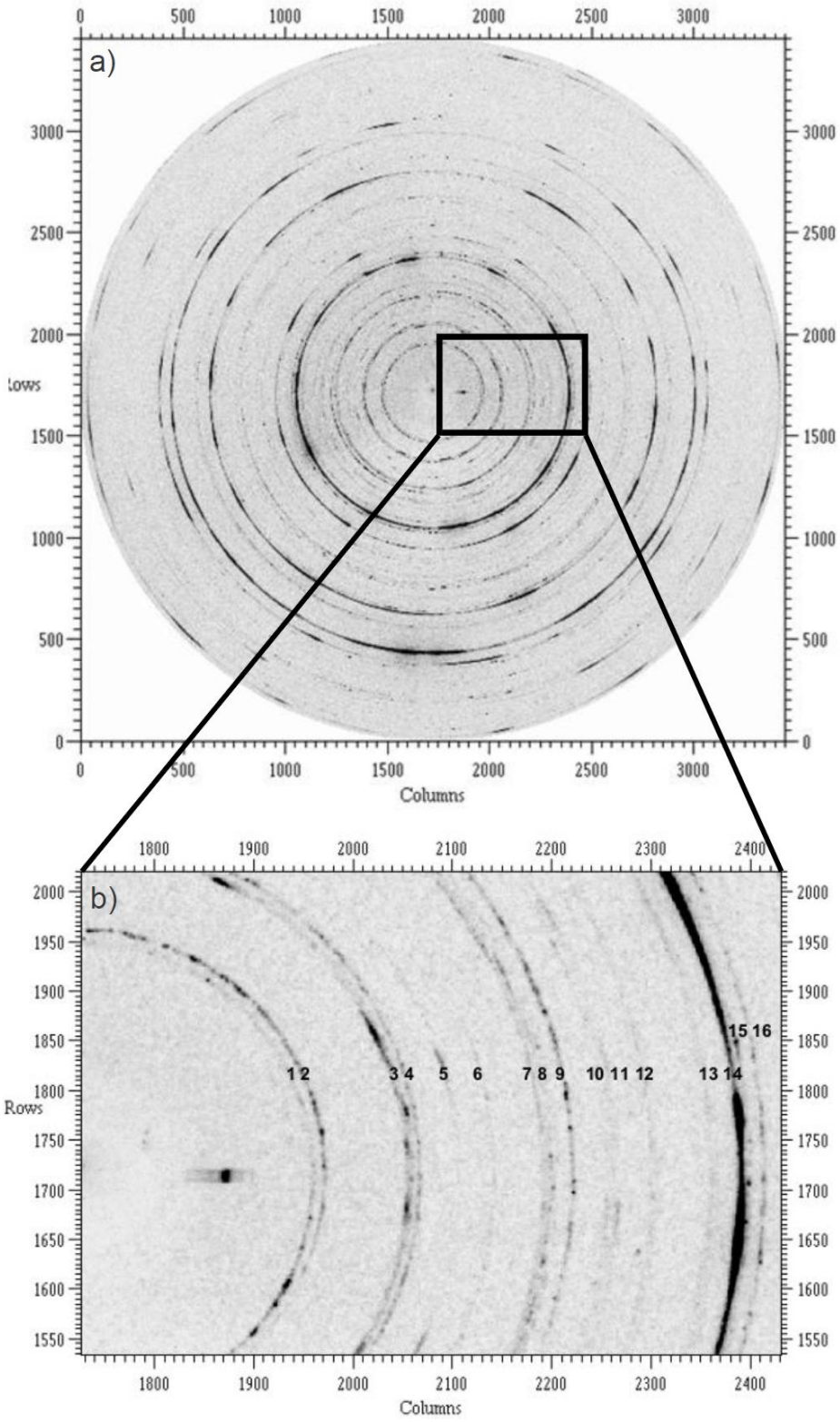

Fig. 3. X-ray synchrotron diffraction of the Cu/(Sn,Ni) diffusion couple produced at 220 °C for 168 hours (a). Central part of the diffraction pattern with low-intensity reflections is presented in (b). The particular rings are numbered from 1–16 and are described in Table 1.

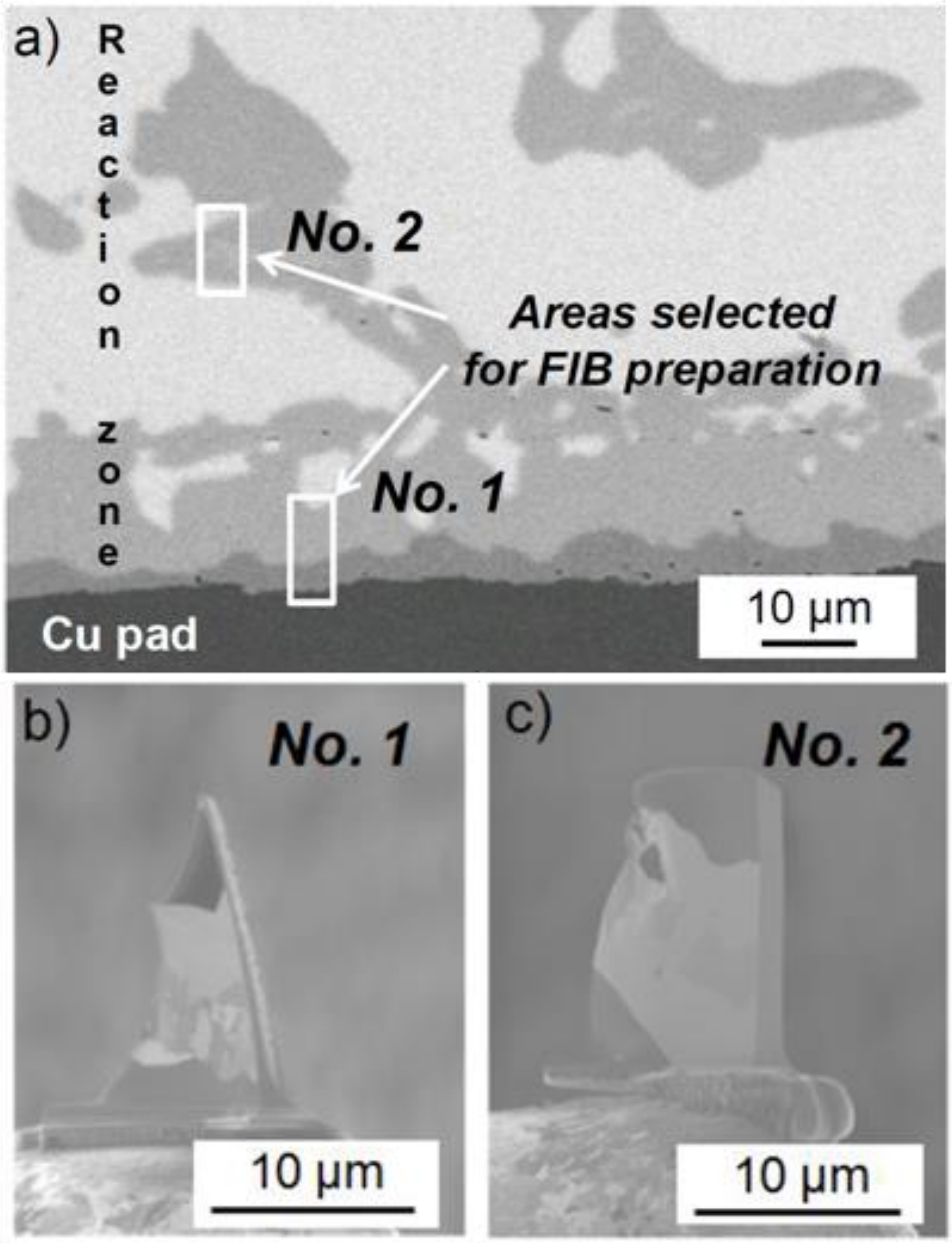

Fig. 4. (a) SEM micrograph of the Cu/(Sn–5 at.%Ni) diffusion couple annealed in a vacuum for 168 hours with the areas chosen for the thin foil preparation together with the lamellas obtained by FIB (b,c).

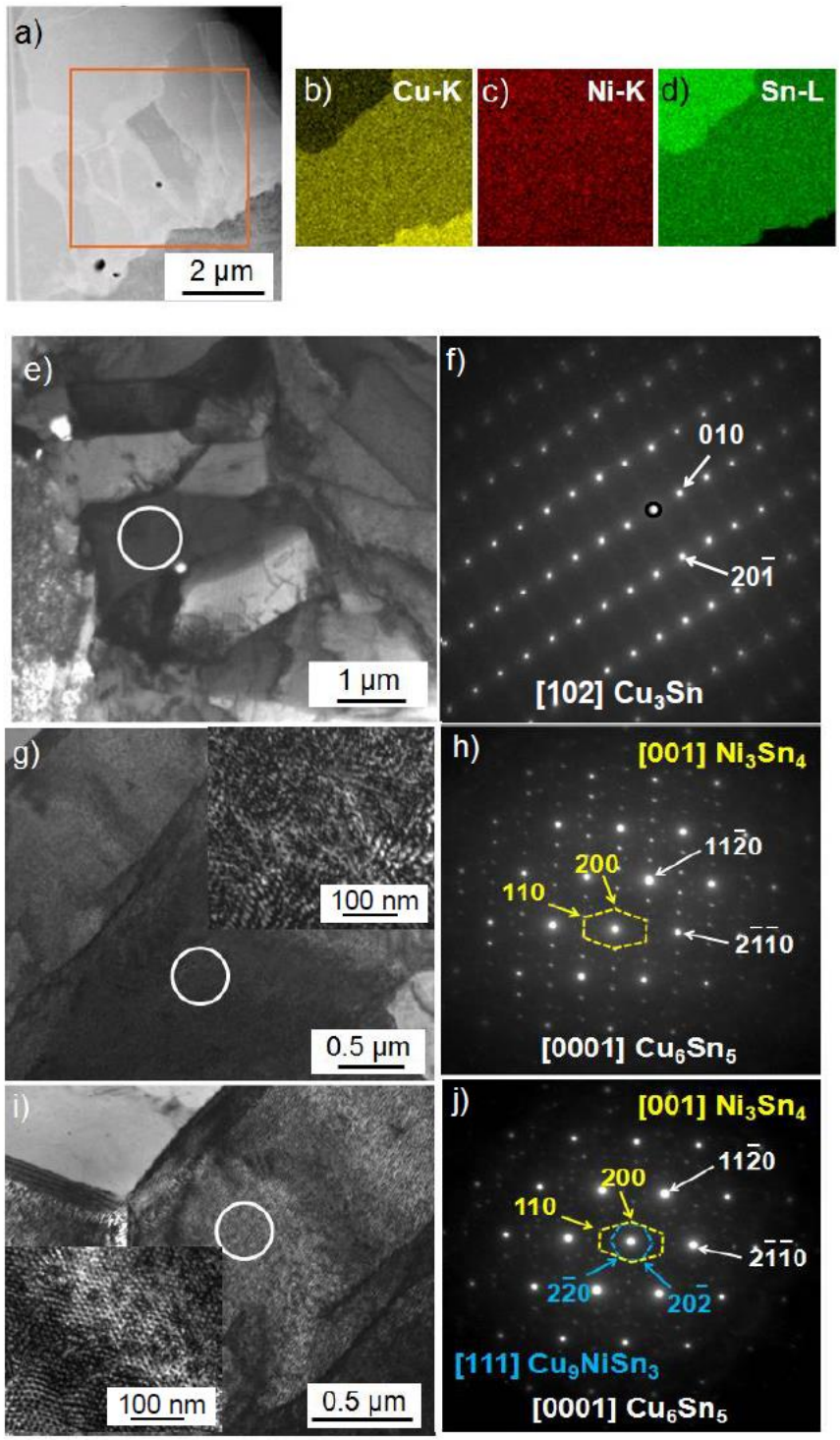

Fig. 5. (a) TEM micrograph of area 1 of the Cu/(Sn+5at.% Ni) diffusion couple annealed in a vacuum for 168 hours and corresponding EDS mapping of (b) Cu, (c) Ni, (d) Sn; (e), (g), (i) bright field images together with their selected area electron diffractions obtained for the areas marked by rings (f), (h), (j).

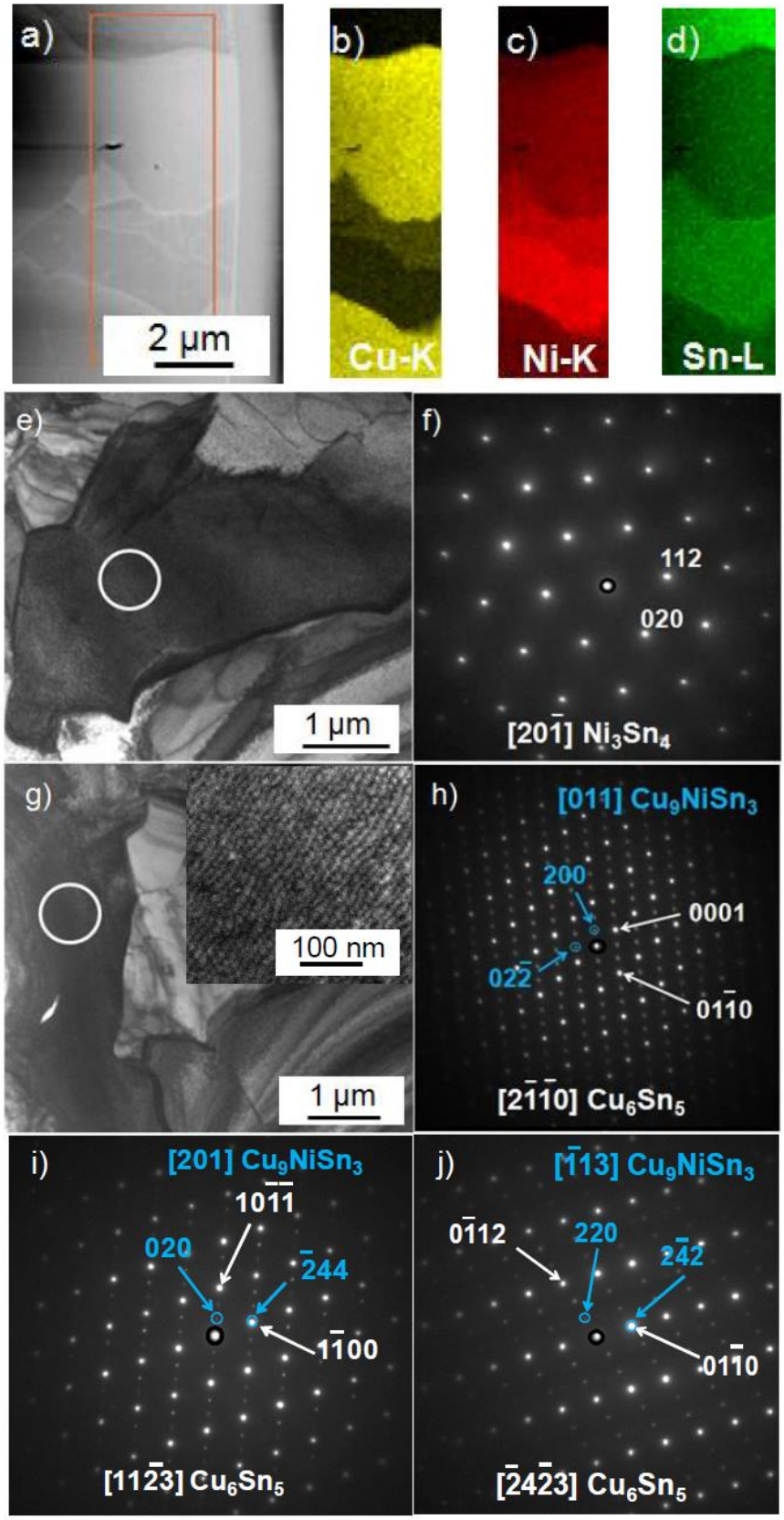

Fig. 6. (a) TEM micrograph of area 2 of the Cu/(Sn+5at.% Ni) diffusion couple annealed in a vacuum for 168 hours and corresponding EDS mapping of (b) Cu, (c) Ni, (d) Sn; (e), (g) bright field images together with their selected area electron diffractions (f), (h).

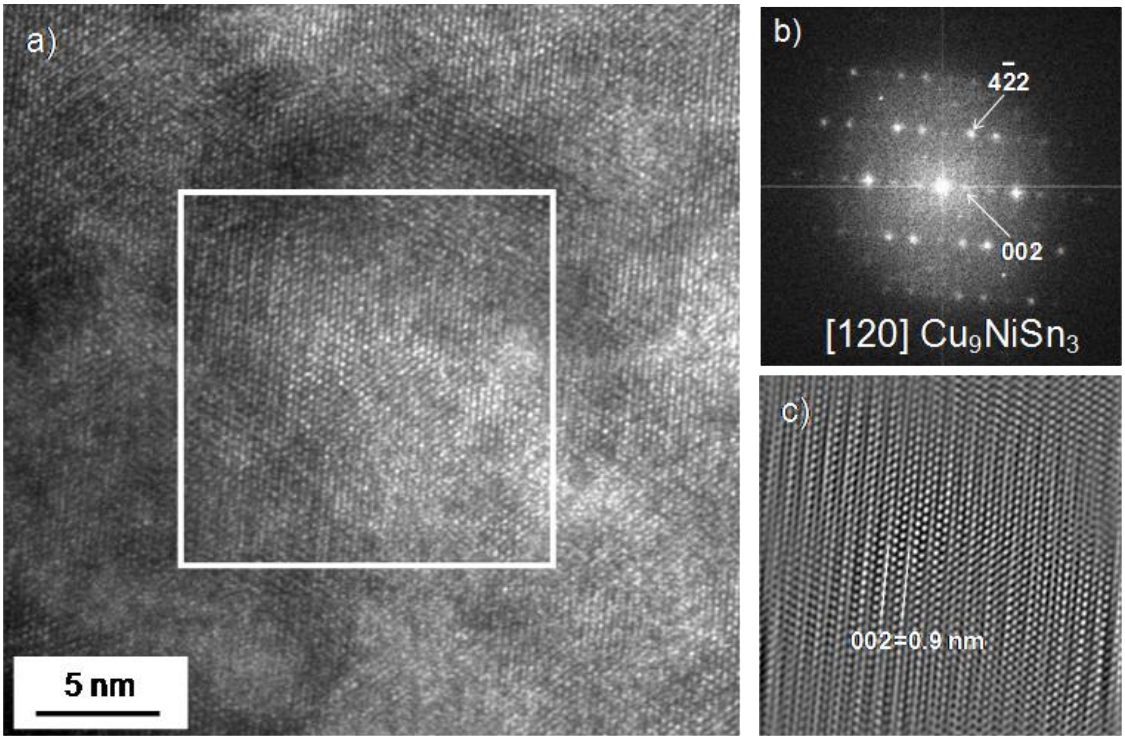

Fig. 7. (a) HRTEM image of Cu_9NiSn_3 phase taken along [120] zone axis, (b) corresponding Fast Fourier Transform and (c) inverse Fast Fourier Transform obtained for the region marked in (a).